Research Article

Yunqi Wang, Chenkai Zhu, Andrew Parsons, Chris Rudd, Ifty Ahmed, and Nusrat Sharmin*

Effects of ZnO addition on thermal properties, degradation and biocompatibility of $P_{45}Mg_{24}Ca_{16}Na_{(15-x)}Zn_x$ glasses

Abstract: Four phosphate-based glass formulations in the system $P_{45}Mg_{24}Ca_{16}Na_{(15-x)}Zn_x$, referred to as P45Znx (x = 0, 5, 10 and 15 mol%), were prepared using a melt quenching process. The effect of ZnO addition on density, molar volume, thermal properties and degradation rates were studied. An increase in the glass transition, crystallisation, melting and liquidus temperatures were seen when replacing Na_2O with ZnO. The molar volume of the bulk glasses was seen to decrease with increasing ZnO content. The dissolution rate of the zinc-free glass was 2.48×10^{-8} kg m^{-2} s^{-1} and addition of 5 mol% ZnO resulted in a reduction of the dissolution rate to 1.68×10^{-8} kg m^{-2} s^{-1}. However, further addition of ZnO from 5 mol% to 15 mol% increased the dissolution rate of the glass system. The glasses were deliberately crystallised and XRD studies identified the $Zn_2P_2O_7$ phase for glass code P45Zn5, and $Zn(PO_3)_2$ phase for P45Zn10 and P45Zn15 glasses. Cytocompatibility studies were conducted using MG63 cells for 14 days. An overall increase in the metabolic activity and DNA concentration of cells was seen from day 1 to day 14 for all glass formulations investigated. However, increasing ZnO content from 0 to 15 mol% seemed to have a negative effect on the cellular activity. Interestingly, a remarkably higher ALP activity was seen at day 14 for glass codes P45Zn5 and P45Zn10 in comparison with the TCP control and the P45Zn0 glass.

Keywords: phosphate glass, ZnO, cytocompatibility, dissolution behaviour, thermal analysis

1 Introduction

Conventional internal fixation metallic biomaterials, such as cobalt-chromium alloys, titanium alloys and stainless steels are inert materials and are known to have drawbacks such as corrosion and release of metal ions, which can cause inflammatory responses in the body [1]. Moreover, the mismatch of mechanical properties between the underlying hard tissues and metallic implants (as the modulus can be more than seven times greater than that of natural bone) can lead to stress shielding, which weakens the underlying bones and increases the rates of refracture after removal of implants [1–4]. Hence, an ideal implant should provide mechanical and structural properties that match the host tissue [5, 6] and allow a gradual transfer of load to the healing bone during the later stages of implantation [6]. Phosphate-based glasses (PBGs) have unique characteristics that would be beneficial as bioresorbable implants for biomedical purposes: (1) their chemical composition is similar to that of the inorganic component of natural bone; (2) they can be dissolved completely in aqueous media (3) their degradation rates can be controlled by simply altering the glass formulations; and these glasses could be drawn into fibres [7, 8]. Therefore, composites made from phosphate glass fibre reinforcements could be an ideal replacement for the metal implants [9, 10]. If applied successfully, removal surgery would not be required, and no inflammatory response would be elicited by the breakdown products [11].

*Corresponding Author: Nusrat Sharmin: Ningbo Nottingham International Academy for the Marine Economy and Technology, University of Nottingham Ningbo China, Ningbo, 315100, China; Ningbo Nottingham New Materials Institute, University of Nottingham Ningbo China, Ningbo, 315100, China; Department of Chemical and Environmental Engineering, University of Nottingham Ningbo China, China; Email: nusrat.sharmin@nottingham.edu.cn
Yunqi Wang: International Doctoral Innovation Centre, University of Nottingham Ningbo China, Ningbo, 315100, China

Chenkai Zhu, Chris Rudd: Ningbo Nottingham International Academy for the Marine Economy and Technology, University of Nottingham Ningbo China, Ningbo, 315100, China; Ningbo Nottingham New Materials Institute, University of Nottingham Ningbo China, Ningbo, 315100, China
Andrew Parsons: Composites Research Group, Faculty of Engineering, University of Nottingham, NG7 2RD, United Kingdom
Ifty Ahmed: Advanced Materials Research Group, Faculty of Engineering, University of Nottingham, Nottingham, NG7 2RD, United Kingdom

Table 1: Classification of PBGs based on the number of BOs.

Types of PBGs	Ultra-	Meta-	Poly-	Pyro-	Invert-	Ortho-
Glass Groups	Q^3; Q^3+Q^2	Q^2	Q^2+Q^1	Q^1	Q^1+Q^0	Q^0
P_2O_5 Content (mol%)	Ultra->50	50	33.3< Poly-<50	33.3	25<Invert-<33.3	25
O/P Ratio	2.5≤ Ultra-<3	3	3<poly-<3.5	3.5	3.5<invert-<4	4

The basic structure of PBGs is composed of phosphate tetrahedra [9, 12]. These tetrahedral units can be classified by the number of bridging oxygen (BO) that are shared with other phosphate tetrahedral and are referred to using the Q^i (i=0, 1, 2, and 3) terminology, where i stands for the number of BOs of an individual phosphate tetrahedron [13]. The structure of phosphate glass can be depolymerised via the addition of modifying oxides. As highly cross-linked phosphate tetrahedra are replaced by those with fewer BOs, the phosphate structural group changes from Q^3 towards Q^0. Meanwhile, the oxygen to phosphorous ratio (O/P) in the glass is increased [14]. Based on the number of BOs with specific components, PBGs can be classified into four types [15–18], which are summarised in Table 1.

The phosphate linkages are susceptible to hydrolysis [19]. It was reported by Parsons *et al.* [20] that ternary phosphate glasses underwent rapid degradation rates and were fully dissolved in aqueous media in hours, thus could not support cell adhesion. Hence, extensive studies have been conducted to improve the cytocompatibility, mechanical and degradation properties of PBGs by adding metal ions such as Mg^{2+} [21–24], Ca^{2+} [25–27], Fe^{3+} [11, 28–30] into the PBG system. These metallic ions can also provide biological benefits to the host [31, 32].

Zinc is a trace element within the human body and is present mainly in the bones with a content of 125-300 ppm [33, 34]. However, zinc is the most widely used metal in biology, and the only metal which contributes to the function of all six enzyme classes, including transferases, oxidoreductases, hydrolases, isomerases, ligases, and lyases [35]. Zinc-containing phosphate glasses have been investigated for their potential use in tissue engineering [36, 37] due to the advantages of zinc ions to the host. Zinc has also been demonstrated extensively to be essential for skeletal growth [38, 39] and to also play a role in the prevention of osteoporosis by stimulating bone mineralization and formation [40–42], increasing bone mineral density [43], and inhibiting bone resorption by inhibiting the formation and activation of osteoclast [44–46]. Moreover, it was reported that zinc ions can stimulate the synthesis of alkaline phosphatase (ALP), which is an important enzyme for bone calcification and DNA synthesis [38, 47, 48].

The cytocompatibility of the glass system $P_{50}Ca_{(40-x)}Na_{10}Zn_x$ has been investigated by both Salih *et al.* [36] (0≤ x≤ 5) and Abou Neel *et al.* [37] (0≤ x≤ 20). The cytocompatibility was seen to improve with increasing zinc content up to 5 mol% [36]. Further addition of ZnO increased the degradation rate [36] and decreased the cytocompatibility [37], which was stated to be associated with the release of significant amount of Zn^{2+} ions, leading to cytotoxicity of the cells [37].

In general, lower phosphate content glasses provide more favourable cell responses, which may be a factor of their degradation profiles (*i.e.* durability and surface stability) [29]. Brauer *et al.* [19] investigated the solubility of glasses in the system of $P_2O_5-CaO-MgO-Na_2O-TiO_2$ and found that with increasing phosphorus oxide content from 35 to 54 mol%, the glass solubility increased due to the glass with longer phosphate chains (*i.e.* with Q^2 and Q^3 groups) being more susceptible to undergoing hydration followed by hydrolysis in solution. Ahmed *et al.* [21] investigated PBG formulations in the system of $P_2O_5-CaO-MgO-Na_2O$ and suggested that the degradation profiles of PBGs with a fixed phosphate content of 40 mol% provided a favourable cytocompatibility response for bone repair applications.

Moreover, the effects of MgO on the chemical durability of the PBG glass were investigated by Franks *et al.* [23] and Lee *et al.* [22]. They both found that substitution of CaO with MgO in the glass systems $P_{45}Ca_{(32-x)}Na_{23}Mg_x$ (0≤ x≤ 22) [23] and $P_{50}Ca_{(30-x)}Na_{20}Mg_x$ (0≤ x≤ 30) [22] improved their chemical durability, due to higher cation field strength of Mg^{2+} in comparison with Ca^{2+} [22]. In addition, Cozien-Cazuc [49] investigated the glass system of $40P_2O_5$-xCaO-(40-x)MgO-$20Na_2O$ and found that the glass fibre of $40P_2O_5$-16CaO-24MgO-$20Na_2O$ maintained maximum mechanical properties after immersing in PBS for 14 days. On the other hand, production of fibres was easier with glasses which had a higher quantity of Q^2 groups due to their long phosphate polymeric chain structure [3]. Therefore, the contents of P_2O_5, MgO and CaO were fixed to 45 mol%, 24 mol% and 16 mol% respectively in the present study to ensure a balance between having a suitable degradation profile for tissue engineering applications, whilst

also maintaining high potential for successful fibre production.

Therefore, the aim of the current study was to investigate the effect of ZnO addition on the thermal, degradation, and biocompatibility properties of novel zinc-containing PBG formulations in the system $P_{45}Mg_{24}Ca_{16}Na_{(15-x)}Zn_x$ (x equals 0, 5, 10 and 15 mol%). The overall goal was to develop PBG compositions with potential to simulate bone formation for hard tissue engineering applications, whilst also retaining properties suitable for fiberisation.

2 Materials and Methods

2.1 Glass preparation

2.1.1 Bulk glass

Four different PBG formulations in the glass system of $P_{45}Mg_{24}Ca_{16}Na_{(15-x)}Zn_x$ (referred to as $P_{45}Zn_x$, where x equals 0, 5, 10 and 15 mol%) were prepared as listed in Table 2. Reagents used to produce the glasses were phosphorous pentoxide (P_2O_5), magnesium hydrogen phosphate trihydrate ($MgHPO_4\cdot3H_2O$), calcium hydrogen phosphate ($CaHPO_4$), sodium dihydrogen phosphate (NaH_2PO_4) (all from Sigma−Aldrich, UK), and zinc carbonate ($Zn_5(CO_3)_2(OH)_6$) (Alfa Aesar). The precursors were mixed in a 200 ml Pt/5% Au crucible (Birmingham Metal Company, U.K.), and preheated at 350°C for 30 minutes to remove any residual H_2O, followed by melting at 1150°C for 90 minutes. Molten glass was then poured onto a steel plate and left to cool to room temperature.

Table 2: The glass composition of zinc-containing PBGs in the system of P45Mg24Ca16Na(15-x)Znx (referred to as P45Znx, where x equals 0, 5, 10 and 15)

Sample Code	P_2O_5 (mol%)	MgO (mol%)	CaO (mol%)	Na_2O (mol%)	ZnO (mol%)
P45Zn0	45	24	16	15	0
P45Zn5	45	24	16	10	5
P45Zn10	45	24	16	5	10
P45Zn15	45	24	16	0	15

2.1.2 Glass rods and discs

A graphite split mould with a cavity diameter of 9 mm was used to make glass rods for the degradation study. The mould was preheated at 450°C for 30 minutes before the molten glass was poured in and held at that temperature for 2 hours. The furnace was then switched off and left to cool to room temperature with the glass inside. The glass rods were annealed in order to remove any potential thermal stress that could cause cracking and breaking during the rod cutting process. During the annealing process, the glass rods were firstly heated to 200°C with a heating rate of 5°C/min, then heated to 10°C above the glass transition temperature (T_g) of the sample (the T_g was determined by DSC) with a heating rate to 1°C/min and held for 90 minutes at this temperature. Afterwards, the furnace was switched off and allowed to cool down to room temperature. The annealed glass rods were cut into 10 mm length cylinders and 2 mm discs for degradation and cell culture studies, respectively, using a low speed diamond wheel saw (South Bay Technologies, California, USA) equipped with a diamond blade (Buehler, Coventry, UK). Ethanol (Fisher Chemicals, UK) was used for lubrication. An ultrasonic cleaner (U300H, Ultrawave Limited, UK) was used to clean the rods and discs.

2.2 X-ray diffraction (XRD)

XRD analysis was used first to confirm the amorphous state of the bulk glasses, then subsequently to determine the crystalline phases for the compositions which had been subjected to crystallisation.

In order to confirm the amorphous nature of the glasses produced, glass samples were ground into powders using an agate pestle and mortar and then compressed using a hand press to create a flat surface for scanning. A Bruker D500 X-ray diffractometer was operated at 40 kW and 40 mA with Ni-filtered CuKα-radiation (λ=0.15418 nm). The diffract-AC software program was used to control the scans. A step-size of 0.05° and a dwell time of 2s from 15 to 100° of the diffraction angle (2θ) were used.

To determine the crystalline phases of deliberately crystallised glass samples, the glasses were heat treated at crystallisation temperatures (T_c, determined from DSC) for 1 hour and then left to cool to room temperature, after which they were ground into powder. The crystallised powders were then analysed using a step size of 0.02° and 3s intervals from 15 to 70°.

2.3 Energy dispersive X-ray (EDX)

Compositions of all the glasses were confirmed by EDX analysis using a scanning electron microscope (SEM) (Philips XL30, UK). Before analysis, pieces of bulk glass were coated with carbon using a vacuum evaporator (Edwards E306, Island). The SEM was operated with an accelerating voltage of 20 kV and spot size of 5. EDX The data was collected with an acquisition rate of ~ 4.5 kcps and a live time of 90 seconds.

2.4 Density and molar volume measurements

Density of the glasses was determined using a helium pycnometer (Gas Pyrometer Accupyc 1330, Micrometrics, USA). The density was measured at room temperature with a relative humidity of ~50%. The pycnometer was calibrated (errors within a range of ±0.05%) using a standard calibration ball with a volume of 3.18551 cm^3. Bubble-free bulk glass specimens (~6 g) were used for the density measurement, which was conducted in triplicate. During the measurement, the pressure of helium was set to 21 psi with a purging time of ~15 minutes. The molar volume for each composition was calculated using Equation 1 [50]:

$$V = \frac{\sum n_i \cdot M_i}{\rho} \quad (1)$$

where, V is the molar volume and ρ is the density of the sample, n_i is the molar fraction and M_i is the molar mass of the component i.

2.5 DSC Analysis

Bulk glass samples of each composition were ground into powder using a mortar and pestle. The glass transition temperature (T_g) of the glasses was determined using a differential scanning calorimeter (DSC, TA instruments DSC Q10, UK). Empty aluminium pans were heated from room temperature to 520°C in argon gas with a heating rate of 20°C min^{-1} as a blank run to obtain a baseline. Glass powders (~15-20 mg) were then heated under the same ramping cycle. The T_g was obtained by extrapolating the onset of change in the endothermic reaction based on the heat flow trace obtained by analyser software (TA Universal Analysis).

The crystallisation temperature (T_c), melting temperature (T_m) and liquidus temperature (T_l) of the glasses were determined using a TA Instruments SDT Q600, UK. Glass samples (~20-25 mg) were subjected to a programmed heating cycle employing the T_g values determined above to introduce a known thermal history. For the first heating cycle, glass samples were heated from room temperature to T_g +10°C with a heating rate of 20 °C min^{-1} in flowing argon gas, held at this temperature for 15 minutes to anneal the glass, then cooled to room temperature at a cooling rate of 20°C min^{-1}. After this the samples were heated again to a temperature of 1200°C with a heating rate of 10°C min^{-1}. A black run was conducted to determine the baseline.

2.6 Degradation study

The degradation study on the glass cylinders with a diameter of 9 mm and a height of 10 mm was conducted in accordance with the standard ISO 10993-13:2010 [51]. Glass rods were immersed in glass vials containing ~30 ml of phosphate buffered saline (PBS) solution (pH value of 7.48 ± 0.01) and kept in an oven at 37°C. At various time points (1, 2, 3, 4, 7, 10, 14, 16, 20, 24, 27 and 31 days), glass rods were taken out from the vials and blot dried with tissue before measuring diameter, length, weight of each rods and the pH of the PBS solution. The PBS solution was changed at each time point. The rate of weight loss of the glass formulations was calculated using Equation 2:

$$Weight\ loss\ per\ area\ = (M_o - M_t)/A \quad (2)$$

where, M_o is the original mass of the sample, in kg; M_t is the sample mass measured at each time point, in kg; A is the surface area of the sample measured at teach time point, in m^3. The data were plotted as weight loss per unit area against degradation time (in seconds). The degradation rates (in kg m^{-2} s^{-1}) of each sample were obtained by determining the slope of this graph.

2.7 Cytocompatibility studies

2.7.1 Cell culture

MG63 cells (human osteosarcoma) were obtained from the European Collection of Cell cultures (ECACC). They were cultured in Complete Dulbecco's Modified Eagle Medium (CDMEM) consisting of DMEM supplemented with 8.6% foetal bovine serum (FBS), 1.7% HEPES buffer, 1.7% antibiotics-antimycotics, 0.86% glutamine, 0.86% nonessential amino acids (Gibco Invitrogen, UK) and 0.13 g/L ascorbic acid (Sigma Aldrich, UK).

Cells were cultured in 75 cm^3 flasks (Falcon, Becton, Dickins and company; UK) at 37°C in a humidified atmosphere with 5% CO_2. Once confluent, the cells were detached from the flask using trypsin-EDTA solution (Hanks Balanced Salt Solution (HBSS) containing 2.5 g/L trypsin and 0.18 g/L EDTA) and centrifuged at 1200 rpm for 4 minutes to produce a cell pellet which was then re-suspended in fresh media. Cell concentration was measured using a haemocytometer and viable cells were identified using trypan blue exclusion via microscopy.

Glass discs of each formulation were immersed in ethanol (100% Fisher Chemicals, UK) and washed using an ultrasonic bath (U300H, Ultrawave Limited, UK), then left under UV light for 1 hour for sterilisation before cell culture. Tissue culture plastic (TCP) was used as a positive control for cell growth. Cells were seeded onto the disc surfaces at a concentration of 40,000 cells/cm^2 and incubated at 37°C in a humidified atmosphere with 5% CO_2 for 1, 3, 7 and 14 days.

2.7.2 SEM Analysis

In order to observe the cell morphology via SEM the samples were washed with warm PBS three times and were fixed by applying a 3% glutaraldehyde in 0.1 M Na-cacodylate buffer for 30 minutes. Fixed samples were then washed twice using 0.2 M Na-cacodylate buffer and covered by 1% osmium tetroxide in PBS for 45 minutes. Samples were dehydrated gradually using ethanol. During dehydration, the concentration of ethanol was increased gradually by 10% each time from 20% to 100% with a dwell time of 5 minutes before being fixed using hexamethyldisilazane (HMDS). The samples were then sputter-coated with platinum and observed via a scanning electron microscope (SEM) (Philips XL30, UK) operated at 10 kV.

2.7.3 Alamar blue assay

At the designated time points, culture medium was removed from the wells and the samples were washed three times using warm PBS. One millilitre of alamar blue solution (1:10 alamar blue: HBSS, Thermo Fisher Scientific Inc., USA) was added into each well and incubated for 80 minutes. 100 µl aliquots from each well were transferred to a 96-well plate in triplicate and fluorescence was determined via an FLx800 plate reader (BioTek Instruments) at 530 nm excitation and 590 nm emission.

2.7.4 DNA quantification

The samples were washed with PBS and cells were lysed using a freeze-thaw technique. DNA standards were prepared using calf thymus DNA (sigma, UK) and TNE buffer (10 mM Tris, 2 M NaCl and 1 mM EDTA in sterile distilled water at pH 7.4) as a diluent. 100 µl of Hoechst stain 33258 was added to each well (1 mg of bis-benzimide 33258 in double distilled water and diluted to 1:50 in TNE buffer) and protected in a light-proof container. 100 µl aliquots of cell lysate were transferred to a 96-well plate and mixed with an extra 100 µl of the Hoechst stain. Fluorescence was determined using an FLx800 plate reader at 360 nm excitation and 460 nm emission. DNA concentrations were derived from a standard curve generated by the software KCjunior.

2.7.5 Alkaline phosphatase activity

Alkaline phosphate (ALP) activity was determined using an alkaline phosphatase assay from Randox (UK). At the required time points, cell media was removed and the samples were washed three times using warm PBS, then 1 ml sterile distilled water was added into each well. Cells were lysed using a freeze-thaw technique three times. A 50 µl aliquot of cell lysate was added to a 96-well plate mixed with 50 µl of the alkaline phosphatase substrate (p-nitrophenyl phosphate in diethanolamine buffer at pH 9.8). Well plates were shaken gently for 5 minutes and the absorbance was measured at wavelengths of 405 nm excitation and 620 nm emissions using an ELx800 plate reader (BioTek Instruments Inc).
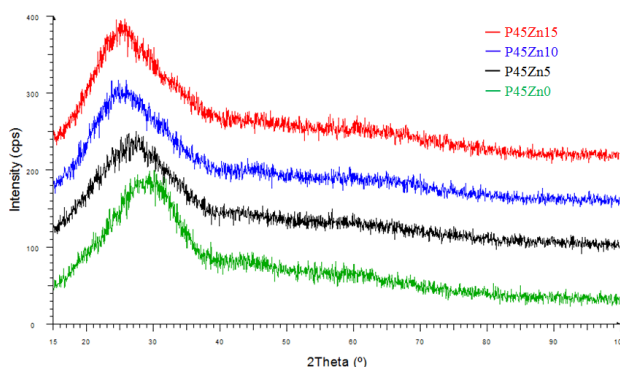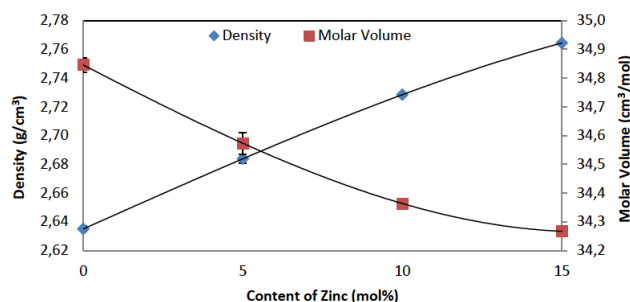
3 Results

3.1 Glass structure and composition

The XRD traces for the glass samples are presented in Figure 1. As can be seen no sharp crystallization peaks were observed, with only a single broad peak between 15° and 40° for all the glass compositions, which suggested that the glasses were amorphous in nature.

The composition of each glass was confirmed using EDX and is listed in Table 3. The differences between the actual and target content of each element were all within a range of ±1.5 mol%.
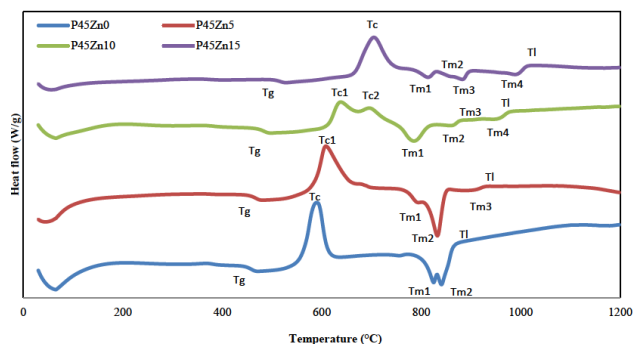
Table 3: Actual compositions of zinc-containing PBGs investigated using EDX

Sample Code	P_2O_5 (mol%)	MgO (mol%)	CaO (mol%)	Na_2O (mol%)	ZnO (mol%)
P45Zn0	45.5 ± 0.1	25.3 ± 0.1	14.9 ± 0.1	14.4 ± 0.1	–
P45Zn5	45.2 ± 0.2	22.7 ± 0.1	17.3 ± 0.1	9.5 ± 0.1	5.3 ± 0.1
P45Zn10	44.6 ± 0.1	23.1 ± 0.1	16.7 ± 0.1	6.2 ± 0.2	9.5 ± 0.1
P45Zn15	44.8 ± 0.1	24.0 ± 0.1	16.4 ± 0.1	–	14.7 ± 0.1

Figure 1: Powder XRD patterns of zinc-containing glasses in the system P45Mg24Ca16Na(15-x)Znx (where x equals 0, 5, 10 and 15)

Figure 2: Plot of density and molar volume of the glasses in the system of P45Mg24Ca16Na(15-x)Znx (where x equals 0, 5, 10 and 15). Lines were drawn as guides for the eye.

3.2 Density and molar volume

The variations in density and molar volume of the glasses with increasing amounts of ZnO are shown in Figure 2. With increasing ZnO content from 0 to 15 mol%, the glass density was seen to increase from 2.64 g/cm^3 to 2.76 g/cm^3 ($P > 0.05$) whilst the molar volume decreased from 34.8 cm^3/mol to 34.3 cm^3/mol ($P > 0.05$).

Figure 3: DSC traces for the P45Mg24Ca16Na(15-x)Znx (referred to as P45Znx, where x equals 0, 5, 10 and 15) glass system.

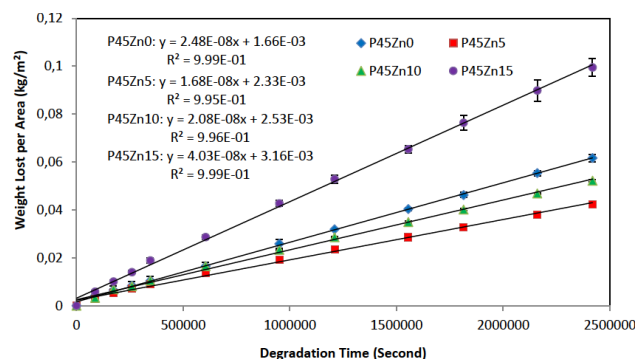## 3.3 Glass transition, crystallization, melting and liquidus temperatures

The thermal traces of the glasses are shown in Figure 3. The corresponding glass transition (T_g), crystallisation (T_c), melting (T_m) and liquidus (T_l) are labelled on the figure as well. T_l was taken to be the temperature at the end of the last melting peak. An increase in T_g from 452°C to 507°C was observed with increasing ZnO content from 0 to 15 mol%. Moreover, broad T_c peaks were observed for the zinc-containing PBG glasses. Two T_c peaks were observed for glass code P45Zn10 at 636°C and 697°C. More than one T_m peak was observed for all the glasses. The two T_m peaks for glass code P45Zn0 were seen at 824°C and 841°C, respectively. In addition, three T_m peaks were seen for glass code P45Zn5, whilst four T_m peaks were observed for both P45Zn10 and P45Zn15 glasses. Additionally, T_l increased from 870°C to 1019°C with increasing ZnO content up to 15 mol%.

3.4 Crystalline Phases

Crystalline phases were determined using XRD analysis to explore the potential role of ZnO within each glass composition. Two main crystalline phases were identified for glass code P45Zn0, and four phases were identified for

Table 4: Phases of crystallized zinc-containing glasses for the P45Mg24Ca16Na(15-x)Znx (referred to as P45Znx, where x equals 0, 5, 10 and 15) glass system.

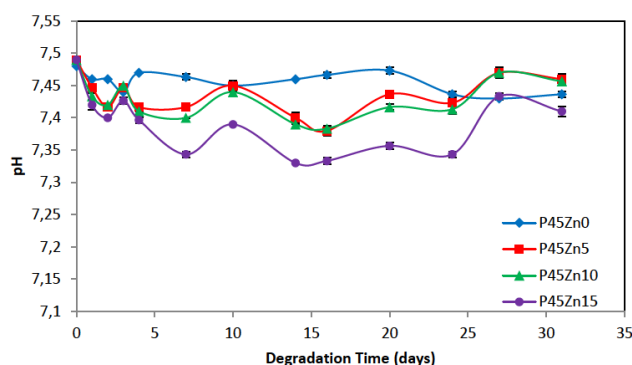| Glass Code	Phase 1	Phase 2	Phase 3	Phase 4
P45Zn0	$NaMg(PO_3)_3$	$Ca_2P_2O_7$		
P45Zn5	$NaMg(PO_3)_3$	$Zn_2P_2O_7$	$Mg_2P_2O_7$	$Ca_{19}Zn_2(PO_4)_{14}$
P45Zn10	$NaMg(PO_3)_3$	$Zn(PO_3)_2$	$Mg(PO_3)_2$	$Ca_{19}Zn_2(PO_4)_{14}$
P45Zn15	$Ca_3(PO_4)_2$	$Zn(PO_3)_2$	$Mg_2P_2O_7$	$Ca_{19}Zn_2(PO_4)_{14}$

Figure 4: The degradation profiles for the glass system P45Mg24Ca16Na(15-x)Znx (referred to as P45Znx, where x equals 0, 5, 10 and 15) in PBS at 37°C for 28 days.

Figure 5: pH profiles for the glass system of P45Mg24Ca16Na(15-x)Znx (referred to as P45Znx, where x equals 0, 5, 10 and 15) in PBS at 37°C for 28 days. Lines were drawn as guides for the eye.

P45Zn5, P45Zn10 and P45Zn15 glasses, as summarized in Table 4.

3.5 Glass solubility

The degradation study was conducted at 37°C for 28 days in PBS solution. Figure 4 shows the degradation profiles of the four glass formulations in terms of weight loss per area (kg/m^2) against degradation time (seconds). It was seen that with increasing ZnO content up to 5 mol% the degradation rate reduced from 2.48×10^{-8} kg m^{-2} s^{-1} to 1.68×10^{-8} kg m^{-2} s^{-1}. However, with further addition of ZnO to 15 mol%, the degradation rate increased (quite significantly) to 4.03×10^{-8} kg m^{-2} s^{-1}.

The pH of the PBS solution was measured at each time point of the degradation study (see Figure 5). The initial pH of the PBS solution was 7.47±0.01 for all glass formulations. The *pH* was seen to decrease ($P > 0.05$) with increasing ZnO content from 0 to 15 mol%. Overlaps of the *pH* profiles for glass code P45Zn5 and P45Zn10 were observed. The minimum *pH* value was seen to be 7.35 ± 0.05 for glass code P45Zn15 at day 7. In general, *pH* values for all the glass formulations remained relatively constant for the duration of the degradation study.

3.6 Cytocompatibility study

3.6.1 Cell morphology

The morphology of the cells cultured on PBG discs was visualized using SEM. The representative SEM images of cells after 1, 3, 7, and 14 days of cell culture are shown in Figure 6. During the initial culture period (day 1) cells adhered to the glass surfaces via the attachment of filopodia and lamellipodia. As the number of cells increased (*i.e.* proliferated), the lamellipodia of cells extended to neighbouring cells. Consequently, a confluent layer of cells formed, which was seen at day 3 for glass codes P45Zn0, P45Zn5 and P45Zn10, and at day 7 for glass code P45Zn15.

A multi-layer of cells was observed for P45Zn0 formulation at day 7, and for both P45Zn5 and P45Zn10 formulations at day 14. In comparison, glass code P45Zn15 had fewer cell clusters during the first three days of culture. Even though, the mature stared shaped structures were observed at day 7, and a confluent layer of cells was observed at day 14.
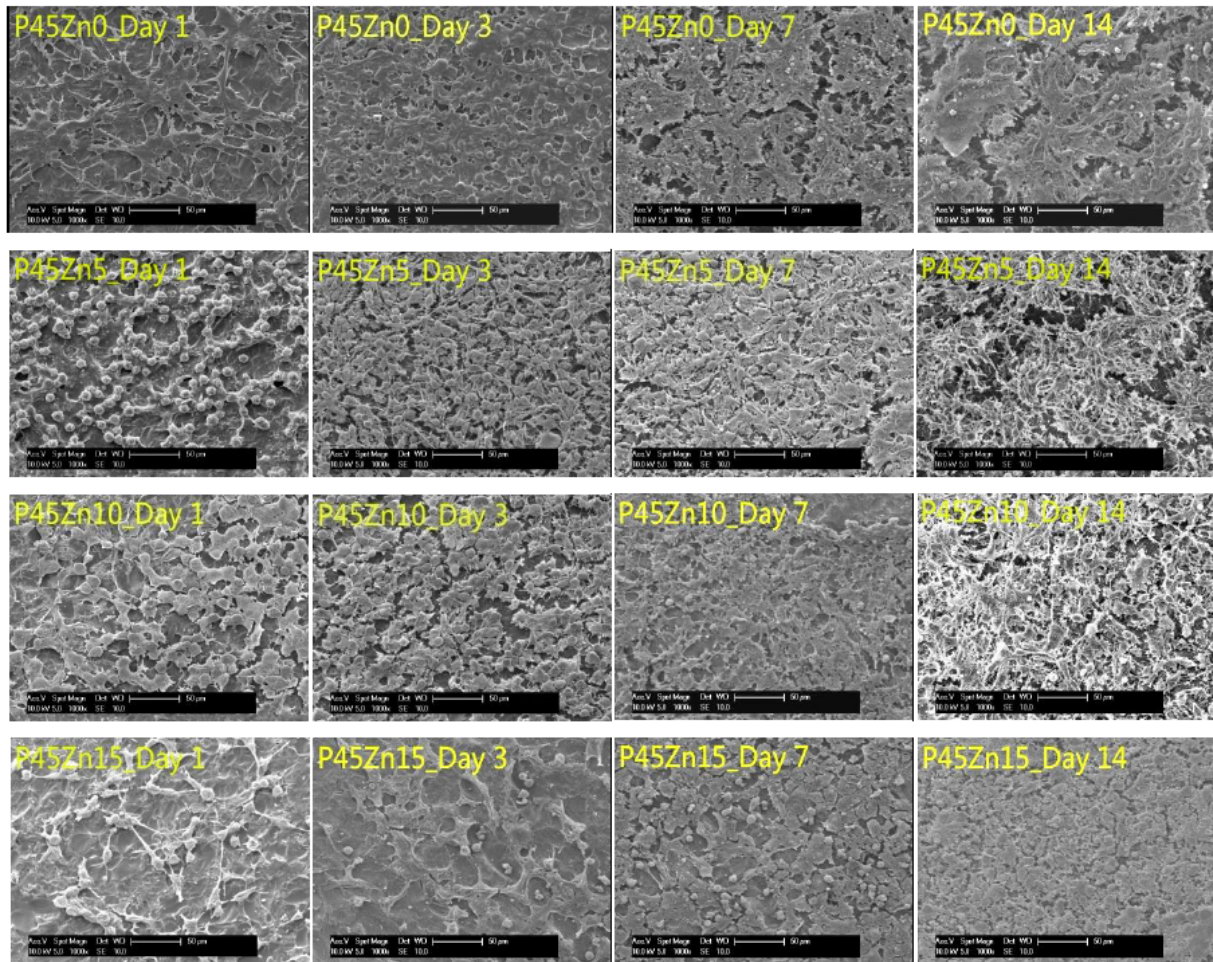
Figure 6: SEM images taken after MG63 cells cultured on the glasses of P45Mg24Ca16Na(15-x)Znx (referred to as P45Znx, where x equals 0, 5, 10 and 15) for 1, 3, 7, and 14 days. The scale bar is 50 μm for all images.

3.6.2 Cell viability/metabolic activity

The effect of ZnO addition on the metabolic activity of osteosarcoma cells (MG63) was investigated using the Alamar Blue assay. Metabolic activity of cells was measured at day 1, 3, 7 and 14 as shown in Figure 7. The metabolic activity of the cells for all the glasses was seen to increase over the duration of cell culture (14 days). At each time point the cell metabolic activity was found to reduce with increasing ZnO content from 0 to 15 mol%. The metabolic activity for P45Zn15 glass was almost undetectable at day 1. Amongst all the glasses investigated, the P45Zn0 glass demonstrated the highest metabolic activity at different time points. In general, the differences in metabolic activity between the glasses and the TCP control decreased over the culture period, especially for the P45Zn0 glass, for which the metabolic activity was seen to be comparable ($P > 0.05$) to the TCP control at day 7 and even became higher ($P > 0.05$) at day 14. Moreover, The P45Zn0 glass showed statistically significant ($P < 0.01$) metabolic activity in comparison with the other zinc-containing glasses throughout the entire culture period. There, the glass formulation with no ZnO showed the best cellular response. However, amongst the zinc-containing glasses, the P45Zn5 glass showed the highest metabolic activity, and even became comparable to that of the TCP control at day 14 ($P > 0.05$).

3.6.3 DNA quantification

The effect of ZnO addition on the proliferation of MG63 cells was evaluated by measuring the DNA quantification of the cells at day 1, 3, 7 and 14 of culture as presented in Figure 8. The DNA concentration was seen to increase throughout the whole culture period for glass codes P45Zn0, P45Zn5, P45Zn10 and the TCP control. However, for the P45Zn15 glass the DNA concentration remained at
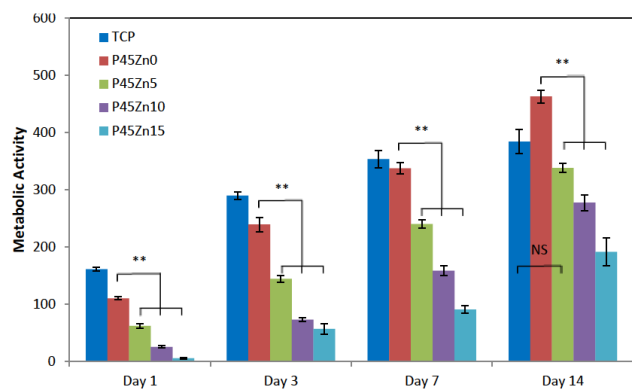
Figure 7: Metabolic activity of MG63 cells cultured on the TCP and glasses of P45Mg24Ca16Na(15-x)Znx (referred to as P45Znx, where x equals 0, 5, 10 and 15) for 1, 3, 7, and 14 days.

Figure 8: DNA quantification of MG63 cells cultured on the TCP and glasses of P45Mg24Ca16Na(15-x)Znx (referred to as P45Znx, where x equals 0, 5, 10 and 15) for 1, 3, 7, and 14 days.
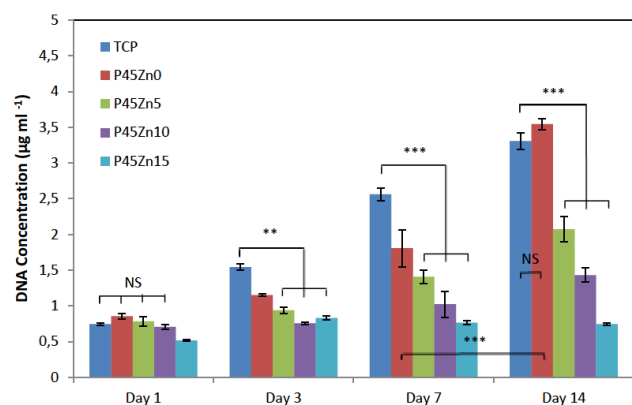

Figure 9: ALP activity of MG63 cells cultured on the TCP and glasses of P45Mg24Ca16Na(15-x)Znx (referred to as P45Znx, where x equals 0, 5, 10 and 15) for 1, 3, 7, and 14 days.

3.6.4 Alkaline phosphatase activity

The effect of ZnO addition on the ALP activity of cells cultured for up to 14 days is presented in Figure 9. No statistically significant difference ($P > 0.05$) in ALP activity was observed for all glass formulations during the initial three days of culture. On day 7, an increase ($P < 0.01$) in ALP activity was seen for the TCP control and the P45Zn5 glass in comparison with day 3, with the P45Zn5 glass showed the highest ALP activity. No significant difference ($P > 0.05$) was observed for the other glass samples on day 7 in comparison with day 1 and 3. On day 14, it was observed that the ALP activity for glass codes P45Zn0, P45Zn5 and P45Zn10 was remarkably higher ($P < 0.001$) than at day 7. Moreover, the ALP activity for the zinc-containing glasses of P45Zn5 and P45Zn10 was observed to be significantly higher ($P < 0.001$) than the TCP control and the P45Zn0 glass. The P45Zn5 glass showed the highest ALP activity since day 7. In addition, the ALP activity of the P45Zn15 glass remained at a similar level throughout the entire culture period. Even so, its ALP activity was comparable ($P > 0.05$) to that of the TCP control at day 14.

4 Discussion

The amorphous nature of the glasses was confirmed for all the samples using XRD (see Figure 1). An increase in glass density was seen with increasing ZnO content up to 15 mol% (see Figure 2). This was suggested to be partly due to the fact that the atomic weight of ZnO (81.39) is higher than that of Na_2O (61.98). A similar trend in density profile was observed by Koudelka *et al.* [52], who replaced ZnO

a level of ~0.5 μgml^{-1} for all the time points. In addition, a decrease in DNA concentration was seen with increasing zinc content up to 15 mol%.

All glass formulations demonstrated similar DNA concentrations at day 1 and the TCP control showed statistically higher concentration of DNA in comparison with the glasses investigated at day 3 and 7 ($P < 0.05$). However, the DNA concentration for the P45Zn0 glass was seen to increase remarkably from 1.8 to 3.5 μgml^{-1} ($P < 0.001$) during the last 7 days of culture, and was higher than the TCP (3.3 μgml^{-1}) at day 14 ($P > 0.05$). For the zinc-containing glasses, DNA concentration was significantly lower ($P < 0.01$) in comparison to the TCP control from day 3 onwards.
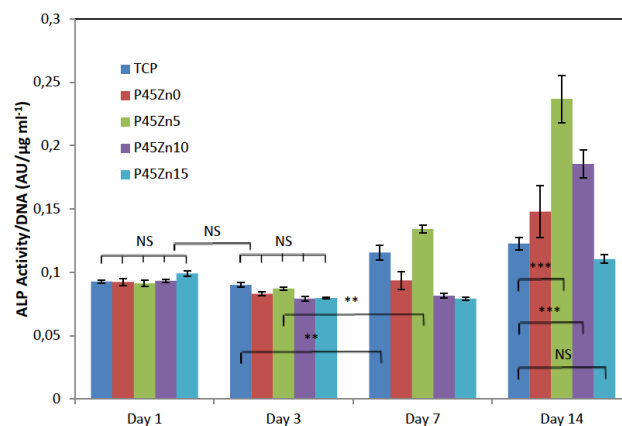
with Li_2O in the PBG glass systems and found a decrease in density with increasing amounts of Li_2O due to the higher atomic weight of ZnO (81.39) as compared to Li_2O (29.88).

The molar volume was seen to decrease with increasing zinc content as seen in Figure 2, indicating a more compact glass system, which also contributed to the increase in the glass density. Moreover, several studies suggest that the addition of modifier oxides normally create more compact glass network due to the ionic cross-linking between the non-bridging oxygens of two different phosphate chains, and these effects seem to manifest for divalent/trivalent modifiers than monovalent modifiers [53, 54]. Omrani *et al.* [55] investigated the glass system (50-x)Na_2O-xZnO-50P_2O_5 (0≤ x≤ 33 mol%), and found that the molar volume decreased with the replacement of Na_2O by ZnO. They also stated that ZnO cross-linked the vitreous network.

The T_g of glass code P45Zn0 (452°C) was comparable with the work done by Parsons *et al.* [56] (450°C) for the same glass composition (referred to as glass code P45Mg24Ca16Na15 in the literature). An increase in T_g was seen in Figure 3 from 452°C to 507°C with increasing ZnO content from 0 to 15 mol%. These results correlated with the work reported by Omrani *et al.* [55]. They investigated the glass system Na_2O-ZnO-P_2O_5 and found a trend of increasing T_g when replacing Na_2O with ZnO. The relative field strengths of the cations, *i.e.* charge/(ionic radius)^2, are often used to explain the variations of glass thermal properties [55, 57]. Hence, the increased T_g of the glass system was mainly due to the substitution of Na ions by Zn ions which have higher ionic field strength [58].

The occurrence of board T_c peaks and several T_m peaks observed for all the glass formulations (see Figure 3) indicated that multiple crystalline phases could potentially be present in that particular glass composition. For instance, multiple T_m peaks and crystalline phases were observed by Ahmed *et al.* [11] who investigated the CaO–Na_2O–Fe_2O_3–P_2O_5 glass system. Two phases were identified as $NaMg(PO_3)_3$ and $Ca_2P_2O_7$ for glass code P45Zn0 (see Table 4), which matched with the two T_m peaks observed from the thermal trace (see Figure 3). The crystalline glass phases of $NaMg(PO_3)_3$, $Zn(PO_3)_2$, $Mg(PO_3)_2$ and $Ca_{19}Zn_2(PO_4)_{14}$ were identified for P45Zn10 glass, and the phases of $Ca_3(PO_4)_2$, $Zn(PO_3)_2$, $Mg_2P_2O_7$ and $Ca_{19}Zn_2(PO_4)_{14}$ were identified for P45Zn15 glass composition (see Table 4). For both glasses, the four crystalline glass phases correlated well with the four T_m peaks exhibited on the thermal traces obtained. However, for P45Zn5 glass, only three T_m peaks were observed, which did not match four glass phases identified by XRD study. This mismatch suggested that either the quantities of some T_m

peaks were too small to be determined by DTA or the T_m peaks of some glass phases were very close and combined together under the same peak [11].

A decrease in the degradation rate of glass system P45Znx from 2.48×10^{-8} kg m^{-2} s^{-1} to 1.68×10^{-8} kg m^{-2} s^{-1} was seen with increasing the content of ZnO from 0 to 5 mol% (see Figure 4). However, an increase was then observed with the addition of the ZnO content from 5 mol% to 15 mol%, which indicated decreased chemical durability of the glass system. This increase in degradation rate was unexpected, since the replacement of a monovalent modifier with a divalent/trivalent modifier, such as CaO [25, 26, 59], MgO [21] and Fe_2O_3 [11, 60], normally improves the chemical durability of the glass system. Ordinarily, these cations are known to increase the cross-links between the non-bridging oxygens of two different phosphate chains and strengthen the glass network [61, 62]. The chemical durability of the glass system P50Ca(40-x)Na10Znx (0≤ x≤ 20) was investigated by Salih *et al.* [36]. They stated that no significant effect on the chemical durability with the addition of ZnO up to 5 mol% was observed, however further addition of ZnO up to 20 mol% significantly impaired the chemical durability of this glass system. Their observations correlated well with the variations of the degradation rate in this work (see Figure 4). They suggested that this chemical durability reduction may due to the Ca-O bonds were replaced with weaker Zn-O bonds. Moreover, zinc ions have a strong polarizing effect on the O ions in the P-O bonds [63], which could result in the weakening of the adjacent P-O bonds [12].

Zinc phosphate glasses have been classified as anomalous because of their unusual discontinuities in composition/property changes (*e.g.* molar volume, the index of refraction, etc.) [64–66]. The anomalies are very pronounced at the metaphosphate composition, which was suggested to be due to the abrupt transition in the coordination number of cations [67]. ZnO is a known intermediate [12]. The actual role of zinc ion in a glass network depends on its coordination state, which can vary from 2 to 6 [68, 69] and it has been stated that zinc could play a role of network former in the four-fold coordination state and act as a typical modifier in the six-fold coordinated state [70].

Takebe *et al.* [71] investigated the dissolution behaviour of binary ZnO-P_2O_5 glasses and found that after the addition of 50-60 mol% of ZnO the crystal $Zn_2P_2O_7·3H_2O$ was precipitated, which correlated well with the determined crystal phase from P45Zn5 glass in this work (see Table 4). It was stated that the zinc ions in the $Zn_2P_2O_7$ compositions were mainly in the six-fold coordinated state and acted as glass network modifiers [75, 79]. Moreover, the chemical durability of their glass system

was seen to be improved with increasing the content of ZnO up to 70 mol% [71], although this improvement could be due to the concomitant replacement of P_2O_5 [19].

With an increase in the content of ZnO in either a binary ZnO-P_2O_5 glass system [72] or ternary ZnO-Na_2O-P_2O_5 glass system [70], the coordination number of the zinc ions decreased from 6 to 4, which resulted in the zinc ions being transformed from a modifier to a network former, with the formation of $[ZnO_4]$ tetrahedra. In the present study, the $Zn(PO_3)_2$ crystal phase was identified from the crystallized glass of both P45Zn10 and 45Zn15 glasses (see Table 4). The coordination numbers of zinc ion in the composition $Zn(PO_3)_2$ was reported to vary from 3 to 6, and four-fold was its main coordination state [67, 68, 73, 74], indicating that ZnO could be acting as a network former in P45Zn10 and 45Zn15 glasses. The $Ca_{19}Zn_2(PO_4)_{14}$ crystalline phase was identified from all zinc-containing PBG formulations, however, limited information about the coordination number of zinc ion in this composition was reported.

Hence, it could be deduced that the role of ZnO transforms from a network modifier to a network former when more than 5 mol% of ZnO was added in the glass system of $P_{45}Mg_{24}Ca_{16}Na_{(15-x)}Zn_x$. Marino *et al.* [75] stated that the role transformation of ZnO from a modifier to a former may lead to a decrease of the O/P ratio of the PBG system (*i.e.* to high Q^i sites). This assumption could be circumstantiated with the work reported by both Koudelka *et al.* [52] and Bioko *et al.* [70], which both investigated the short-range order structural changes of ^{31}P using magic angle spinning nuclear magnetic resonance (MAS NMR). Koudelka *et al.* [52] investigated the glass systems of xLi_2O-$(50-x)ZnO$-$50P_2O_5$, xLi_2O-$(50-x)ZnO$-$10B_2O_3$-$40P_2O_5$ and xLi_2O-$(50-x)ZnO$-$20B_2O_3$-$30P_2O_5$ ($0 \le x \le 50$). They found that the higher content of ZnO, the higher Q^i sites could be determined for all glass systems. Bioko *et al.* [70] investigated the structures of pyrophosphate glasses of $2Na_2O$-P_2O_5, ZnO-Na_2O-P_2O_5, $1.34ZnO$-$0.66Na_2O$-P_2O_5 and $2ZnO$-P_2O_5. They also found that the Q^i distribution was shifted upfield progressively from Q^2 and Q^1 sites to Q^3 and Q^2 sites with increasing the content of ZnO. As mentioned before, the chemical shift of ^{31}P to higher Q^i sites could result in the reduction of chemical durability of the PBG system [19, 76].

Additionally, the bond strength (in kJ/mol) of Zn-O (159.4) bond is much lower than that of P-O (599.1) or Na-O (256.1) [77]. Yang *et al.* [63] investigated the glass system of $(20-x)Li_2O$-$xZnO$-$30Fe_2O_3$-$50P_2O_5$ with a ZnO content up to 7.2 mol%. They found that with adding 2 mol% of ZnO into the glass system, zinc ions cross-linked the phosphate chains by forming P-O-Zn bridges, however, further

addition of ZnO resulted in the formation of $[ZnO_4]$ tetrahedra. They suggested that the formation of $[ZnO_4]$ improved the integration of the glass system and consequently contributed to the accretion of the glass density. Even though, they also stated that ZnO would have negative effects to the glass system: the bonding energy of Zn-O bond is smaller than P-O bond, whereas the volume of $[ZnO_4]$ tetrahedron is larger than the $[PO_4]$ tetrahedron.

Therefore, it could be deduced that the reduction of the chemical durability of the bulk glass seen in this study was due mainly to the role of ZnO transforming from a network modifier to a former when adding more than 5 mol% of ZnO.

Amongst all the zinc-containing PBGs, the glass code P45Zn5 showed the highest metabolic activity. It was comparable ($P > 0.05$) to that of TCP control at day 14, however remained lower ($P < 0.01$) than the P45Zn0 glass. The DNA quantification, which reflected the amount of cells, showed a similar profile to the cell metabolic study, with DNA quantification for the TCP control being significantly higher ($P < 0.01$) than the zinc-containing glasses from day 3 onwards (see Figure 8). A stimulation effect of Zn ions on the ALP activity was seen from day 7 (see Figure 9). The ALP activity for P45Zn5 and P45Zn10 glasses increased significantly ($P < 0.001$) during the last seven days of culture. The highest ALP activity was seen for glass code P45Zn5 at day 14 with the ALP activity being twice that of the TCP control, indicating a stimulation effect on ALP activity of cells in comparison with zinc-free samples.

The cytotoxicity of a biodegradable material depends partly on the concentration of ions released during degradation [78]. Although there were several studies that report the benefits of zinc for bone formation, the limit of beneficial effect should be considered. Additionally, cell adhesion, proliferation and death could also be influenced by *pH* [79]. It was reported that the activity of human osteoblasts increased with increasing pH value within a range of 7.0 to 7.6 [80]. This phenomenon was further confirmed by the biocompatibility tests in this study, which showed that the glass with higher *pH* value (see Figure 5) during degradation achieved a higher cell metabolic activity (see Figure 7) and proliferation (see Figure 8).

Hence, it was concluded that the metabolic activity and proliferation of cells reduced with increasing the content of ZnO could be due to the reduced pH value and the high concentration of Zn^{2+} released from the glass system during cell culture, and may consequently depress or even have a toxic effect on the proliferation of cells. This deduction correlated well with the biocompatibility studies of the glass system of $P_{50}Ca_{(40-x)}Na_{10}Zn_x$ reported by both Salih *et al.* [36] ($0 \le x \le 5$) and Abou Neel *et al.* [37] ($0 \le x \le 20$).

They found that the cell proliferation increased with increasing the zinc content from 0 to 5 mol%, whereas further addition of ZnO to 10-20 mol% resulted in a remarkable reduction of glass biocompatibility due to the release of significant amount of zinc and hydrogen ions, which have a toxic effect on MG63 cells. Therefore, it was suggested the addition of ZnO should not exceed 5 mol% for the glass system $P_{45}Mg_{24}Ca_{16}Na_{(15-x)}Zn_x$ in order to stimulate ALP production while avoiding the toxic effects.

5 Conclusion

ZnO was found to provide both beneficial and adverse effects on the properties of the glasses investigated in this study. On the one hand the replacement of monovalent Na^+ ion with the higher field strength Zn^{2+} increased the thermal properties (*i.e.* T_g, T_s, T_f and T_l). On the other hand, when the addition of a particular amount of ZnO was exceeded (*i.e.* more than 5 mol% in the present research) the chemical durability of the glasses were seen to decrease. This was in agreement with other studies in the literature.

As the chemical durability of the glass decreased with increasing ZnO content (degradation rate increased), cell attachment and proliferation reduced. However, zinc-containing PBGs showed a stimulatory effect on ALP activity in comparison with zinc-free samples. From its biological performance, it was suggested the P45Zn5 glass was the most desirable formulation in this study and could potentially be used for hard tissue engineering.

Conflict of Interests: Authors state no conflict of interest.

Ethical approval: The conducted research is not related to either human or animals use

References

[1] Patel, N.R. and P.P. Gohil, *A Review on Biomaterials: Scope, Applications & Human Anatomy Significance*. International Journal of Emerging Technology and Advanced Engineering, 2012. **2**(4):

p. 91-101.

[2] Hench, L.L., *Biomaterials*. Science, 1980. **208**: p. 826-831.

[3] Knowles, J.C., *Phosphate based glasses for biomedical applications*. Journal of Materials Chemistry, 2003. **13**(10): p. 2395-2401.

[4] Parsons, A.J., et al., *Phosphate Glass Fibre Composites for Bone Repair*. Journal of Bionic Engineering, 2009. **6**(4): p. 318-323.

[5] Wang, M., *Developing bioactive composite materials for tissue replacement*. Biomaterials, 2003. **24**(13): p. 2133-2151.

[6] Gerhardt, L.-C. and A.R. Boccaccini, *Bioactive Glass and Glass-Ceramic Scaffolds for Bone Tissue Engineering*. Materials, 2010. **3**(7): p. 3867-3910.

[7] Sharmin, N., et al., *Effect of boron oxide addition on fibre drawing, mechanical properties and dissolution behaviour of phosphate-based glass fibres with fixed 40, 45 and 50 mol% P2O5*. J Biomater Appl, 2014. **29**(5): p. 639-53.

[8] Sharmin, N., et al., *Effect of Boron Addition on the Thermal, Degradation, and Cytocompatibility Properties of Phosphate-Based Glasses*. BioMed Research International, 2013. **2013**: p. 12.

[9] Nusrat Sharmin, C.D.R., *Structure, thermal properties, dissolution behaviour and biomedical applications of phosphate glasses and fibres: a review*. Journal of Materials Science, 2017. **52**(15): p. 8733-8760.

[10] Sharmin, N., et al., *Cytocompatibility, mechanical and dissolution properties of high strength boron and iron oxide phosphate glass fibre reinforced bioresorbable composites*. Journal of the Mechanical Behavior of Biomedical Materials, 2016. **59**: p. 41-56.

[11] Ahmed, I., et al., *Processing, characterisation and biocompatibility of iron-phosphate glass fibres for tissue engineering*. Biomaterials, 2004. **25**(16): p. 3223-32.

[12] Hoppe, U., *A structural model for phosphate glasses*. Journal of Non-Crystalline Solids, 1996. **195**: p. 138-147.

[13] Abou Neel, E.A., et al., *Bioactive functional materials: a perspective on phosphate-based glasses*. Journal of Materials Chemistry, 2009. **19**(6): p. 690.

[14] Kirkpatrick, R.J. and R.K. Brow, *Nuclear magnetic resonance investigation of the structures of phosphate and phosphate-containing glasses: a review*. Solid State Nuclear Magnetic Resonance, 1995. **5**: p. 9-21.

[15] Brow, R.K., *Review: the structure of simple phosphate glasses*. Journal of Non-Crystalline Solids, 2000. **263&264**: p. 1-28.

[16] Walter, G., et al., *The Structure of CaO-Na$_2$O-MgO-P$_2$O$_5$ Invert glass*. Journal of Non-Crystalline Solids, 2001. **296**: p. 212-223.

[17] Brow, R.K., C.A. Click, and T.M. Alam, *Modifier coordination and phosphate glass networks*. Journal of Non-Crystalline Solids, 2000. **274**: p. 9-16.

[18] Tischendorf, B., et al., *A study of short and intermediate range order in zinc phosphate glasses*. Journal of Non-Crystalline Solids, 2001. **282**: p. 147-158.

[19] Brauer, D.S., C. Rüssel, and J. Kraft, *Solubility of glasses in the system P2O5−CaO−MgO−Na2O−TiO2: Experimental and modeling using artificial neural networks*. Journal of Non-Crystalline Solids, 2007. **353**(3): p. 263-270.

[20] Parsons, A.J., et al., *Synthesis and degradation of sodium iron phosphate glasses and their in vitro cell response*. J Biomed Mater Res A, 2004. **71**(2): p. 283-91.

[21] Ahmed, I., et al., *Cytocompatibility and effect of increasing MgO content in a range of quaternary invert phosphate-based glasses*. J Biomater Appl, 2010. **24**(6): p. 555-75.

[22] Lee, I.-H., et al., *Effects of magnesium content on the physical, chemical and degradation properties in a MgO-CaO-Na2O-P2O5*

glass system. Journal of Non-Crystalline Solids, 2013. **363**: p. 57-63.

[23] Franks, K., et al., *The effect of MgO on the solubility behavior and cell proliferation in a quaternary soluble phosphate based glass system.* Journal of Materials Science: Materials in Medicine, 2002. **13**: p. 549-556.

[24] Tamimi, F., et al., *Biocompatibility of magnesium phosphate minerals and their stability under physiological conditions.* Acta Biomater, 2011. **7**(6): p. 2678-85.

[25] Ahmed, I., et al., *Phosphate glasses for tissue engineering: Part 1. Processing and characterisation of a ternary-based P2O5−CaO−Na2O glass system.* Biomaterials, 2004. **25**(3): p. 491-499.

[26] Ahmed, I., et al., *Comparison of phosphate based glasses in the range 50P2O5-(50-x)CaO- xNa2O prepared using different precursors* Journal of Glass Science and Technology, A, 2008. **49**(2): p. 63-72.

[27] Salih, V., et al., *Development of soluble glasses for biomedical use Part II: The biological response of human osteoblase cell lines to phosphate-based soluble glasses.* Journal of Materials Science: Materials in Medicine, 2000. **11**: p. 615-620.

[28] Parsons, A.J. and C.D. Rudd, *Glass forming region and physical properties in the system P2O5-Na2O-Fe2O3.* Journal of Non-Crystalline Solids, 2008. **354**(40-41): p. 4661-4667.

[29] Hasan, M.S., et al., *Material characterisation and cytocompatibility assessment of quinternary phosphate glasses.* J Mater Sci Mater Med, 2012. **23**(10): p. 2531-41.

[30] Haque, P., et al., *Degradation properties and microstructural analysis of 40P2O5−24MgO−16CaO−16Na2O−4Fe2O3 phosphate glass fibres.* Journal of Non-Crystalline Solids, 2013. **375**: p. 99-109.

[31] Hoppe, A., N.S. Guldal, and A.R. Boccaccini, *A review of the biological response to ionic dissolution products from bioactive glasses and glass-ceramics.* Biomaterials, 2011. **32**(11): p. 2757-74.

[32] Mourino, V., J.P. Cattalini, and A.R. Boccaccini, *Metallic ions as therapeutic agents in tissue engineering scaffolds: an overview of their biological applications and strategies for new developments.* J R Soc Interface, 2012. **9**(68): p. 401-19.

[33] Grynpas, M.D., K.P.H. Pritzker, and R.G.V. Hancock, *Neutron activation analysis of bulk and selected trace elements in bone using low flux SLOWPOKE reactor.* Biological Trace Element Research, 1987. **13**(1): p. 333-344.

[34] Ito, A., et al., *Zinc-containing tricalcium phosphate and related materials for promoting bone formation.* Current Applied Physics, 2005. **5**(5): p. 402-406.

[35] Vallee, B.L. and K.H. Falchuk, *The Biochemical Basis of Zinc Physiology.* Physiological Reviews, 1993. **73**(1): p. 79-118.

[36] Salih, V., A. Patel, and J.C. Knowles, *Zinc-containing phosphate-based glasses for tissue engineering.* Biomed Mater, 2007. **2**(1): p. 11-20.

[37] Abou Neel, E.A., et al., *Processing, characterisation, and biocompatibility of zinc modified metaphosphate based glasses for biomedical applications.* J Mater Sci Mater Med, 2008. **19**(4): p. 1669-79.

[38] Yamaguchi, M. and R. Yamaguchi, *ACTION OF ZINC ON BONE METABOLISM IN RATS.* Biochemical Pharmacology, 1986. **35**(5): p. 773-777.

[39] Ovesen, J., et al., *The Positive Effects of Zinc on Skeletal Strength in rats.* Bone, 2001. **29**(6): p. 565-570.

[40] Yamaguchi, M., H. Oishi, and Y. Suketa, *Stimulatory effect of zinc on bone formation in tissue culture.* Biochemical Pharmacology, 1987. **36**(22): p. 4007-4012.

[41] Matsui, T. and M. Yamaguchi, *Zinc Modulation of Insulin-Like Growth Factor's effect in osteoblastic MC3T3-E1 cells.* Peptides, 1995. **16**(6): p. 1063-1068.

[42] Luo, X., et al., *Zinc in calcium phosphate mediates bone induction: in vitro and in vivo model.* Acta Biomater, 2014. **10**(1): p. 477-85.

[43] Angus, R.M., et al., *Dietary intake and bone mineral density.* Bone & Mineral, 1988. **4**(3): p. 265-77.

[44] Yamaguchi, M., *Role of Zinc in Regulation of Osteoclastogenesis.* Biomed Res Trace Elements, 2004. **15**(1): p. 9-14.

[45] Wang, T., et al., *Effect of zinc ion on the osteogenic and adipogenic differentiation of mouse primary bone marrow stromal cells and the adipocytic trans-differentiation of mouse primary osteoblasts.* J Trace Elem Med Biol, 2007. **21**(2): p. 84-91.

[46] Kishi, S. and M. Yamaguchi, *Inhibitory effect of zinc compounds on osteoclast-like cell formation in mouse marrow cultures.* Biochemical Pharmacology, 1994. **48**(6): p. 1225-1230.

[47] Dimai, H.P., et al., *Skeletal Response to Dietary Zinc in Adult Female Mice.* Calcified Tissue International, 1998. **62**(4): p. 309-315.

[48] Hall, S.L., H.P. Dimai, and J.R. Farley, *Effects of zinc on human skeletal alkaline phosphatase activity in vitro.* Calcified Tissue International, 1999. **64**(2): p. 163-72.

[49] Cozien-Cazuc, S., *CHARACTERISATION OF RESORBABLE PHOSPHATE GLASS FIBRES*, in *School of Mechanical, Materials and Manufacturing Engineering*. 2006, The University of Nottingham: Nottingham, UK. p. 23-79.

[50] Toyoda, S., S. Fujino, and K. Morinaga, *Density, viscosity and surface tension of 50RO−50P2O5 (R: Mg, Ca, Sr, Ba, and Zn) glass melts.* Journal of Non-Crystalline Solids, 2003. **321**(3): p. 169-174.

[51] *Biological evaluation of medical devices. Part 13: Identification and quantification of degradation products from polymeric medical devices.* International standard. ISO 10993-13:2010.

[52] Koudelka, L., et al., *Study of lithium−zinc borophosphate glasses.* Journal of Materials Science, 2006. **41**(14): p. 4636-4642.

[53] Walter, G., et al., *Intermediate range order in MeO-P2O5 glasses.* Journal of Non Crystalline Solids, 1997. **217**(2-3): p. 299-307.

[54] Bingham, P.A., et al., *Effects of modifier additions on the thermal properties, chemical durability, oxidation state and structure of iron phosphate glasses.* Journal of Non-Crystalline Solids, 2009. **355**(28-30): p. 1526-1538.

[55] Omrani, R.O., et al., *Structural and thermochemical study of Na2O−ZnO−P2O5 glasses.* Journal of Non-Crystalline Solids, 2014. **390**: p. 5-12.

[56] Parsons, A.J., et al., *Viscosity profiles of phosphate glasses through combined quasi-static and bob-in-cup methods.* Journal of Non-Crystalline Solids, 2015. **408**: p. 76-86.

[57] Smith, C.E. and R.K. Brow, *The properties and structure of zinc magnesium phosphate glasses.* Journal of Non-Crystalline Solids, 2014. **390**: p. 51-58.

[58] Montagne, L., G. Palavit, and R. Delaval, *31p NMR in (100 - x)(NaPO 3) -xZnO glasses.* Journal of Non-Crystalline Solids, 1997. **215**: p. 1-10.

[59] Delahaye, F., et al., *Acid dissolution of sodium-calcium metaphosphate glasses.* Journal of Non-Crystalline Solids, 1998. **242**: p. 25-32.

[60] Abou Neel, E.A., et al., *Effect of iron on the surface, degradation and ion release properties of phosphate-based glass fibres.* Acta Biomater, 2005. **1**(5): p. 553-63.

[61] Bunker, B.C., G.W. Arnold, and J.A. Wilder, *Phosphate glass dissolution in aqueous solutions* Journal of Non-Crystalline Solids, 1984. **64**: p. 291-316.

[62] Muñoz-Senovilla, L. and F. Muñoz, *Behaviour of viscosity in metaphosphate glasses.* Journal of Non-Crystalline Solids, 2014. **385**: p. 9-16.

[63] Yang, R., et al., *Structure and properties of ZnO-containing lithium–iron–phosphate glasses.* Journal of Alloys and Compounds, 2012. **513**: p. 97-100.

[64] STACHEL, D., et al., *STRUCTURAL RELATIONS BETWEEN CRYSTALLINE AND GLASSY PHOSPHATES.* Phosphorus Research Bulletin, 1999. **10**: p. 503-508.

[65] Sales, B.C., et al., *Structure of zinc polyphosphate glasses.* Journal of Non-Crystalline Solids, 1998. **226**: p. 287-293.

[66] Brow, R.K., et al., *The short-range structure of zinc polyphosphate glass.* Journal of Non-Crystalline Solids, 1995. **191**: p. 45-55.

[67] Matz, W., D. Stachel, and E.A. Goremychkin, *The structure of alkaline earth metaphosphate glasses investigated by neutron diffraction.* Journal of Non-Crystalline Solids, 1988. **101**(1): p. 80-89.

[68] Tischendorf, B.C., et al., *The structure and properties of binary zinc phosphate glasses studied by molecular dynamics simulations.* Journal of Non-Crystalline Solids, 2003. **316**: p. 261-272.

[69] Walter, G., et al., *The structure of zinc polyphosphate glass studied by diffraction methods and 31P NMR.* Journal of Non-Crystalline Solids, 2004. **333**(3): p. 252-262.

[70] Boiko, G.G., N.S. Andreev, and A.V. Parkachev, *Structure of pyrophosphate 2ZnO · P2O5–2Na2O · P2O5 glasses according to molecular dynamics simulation.* Journal of Non-Crystalline Solids, 1998. **238**: p. 175-185.

[71] Takebe, H., Y. Baba, and M. Kuwabara, *Dissolution behavior of ZnO–P2O5 glasses in water.* Journal of Non-Crystalline Solids, 2006. **352**(28-29): p. 3088-3094.

[72] Hoppe, U., et al., *The dependence of structural peculiarities in binary phosphate glasses on their network modifier content.* Journal of Non-Crystalline Solids, 1995. **192 & 193**: p. 28-31.

[73] Sourial, E., et al., *A structural investigation of Mg(PO3)2, Zn(PO3)2 and Pb(PO3)2 glasses using molecular dynamics simulation.* Physical Chemistry Chemical Physics, 1999. **1**(8): p. 2013-2018.

[74] Navarra, G., et al., *The structure of a zinc metaphosphate glass. A reverse Monte Carlo study.* Physical Chemistry Chemical Physics, 2002. **4**(19): p. 4817-4822.

[75] Marino, A.E., et al., *Durable phosphate glasses with lower transition temperatures.* Journal of Non-Crystalline Solids, 2001. **289**: p. 37-41.

[76] Parsons, A.J., et al., *Properties of sodium-based ternary phosphate glasses produced from readily available phosphate salts.* Journal of Non-Crystalline Solids, 2006. **352**(50-51): p. 5309-5317.

[77] Lide, D.R., *CRC handbook of chemistry and physics.* 2005, Boca Raton, FL: CRC Press.

[78] Yamanoto, A., R. Honma, and M. Sumita, *Cytotoxicity evaluation of 43 metal salts using murine fibroblasts and osteoblastic cells.* Journal of Biomedical Materials, 1998. **39**: p. 331-340.

[79] Skelton, K.L., et al., *Effect of ternary phosphate-based glass compositions on osteoblast and osteoblast-like proliferation, differentiation and death in vitro.* Acta Biomater, 2007. **3**(4): p. 563-72.

[80] Kaysinger, K.K. and W.K. Ramp, *Extracellular pH Modulates the Activity of Cultured Human Osteoblasts.* journal of Cellular Biochemistry, 1998. **68**: p. 83-89.